Article

Analysis of chaotic dynamics: A fractional order glycolysis model

Md. Jasim Uddin, **S. M. Sohel Rana**
Department of Mathematics, University of Dhaka, Dhaka-1000, Bangladesh
E-mail: jasim.uddin@du.ac.bd, srana_math@du.ac.bd

Received 12 August 2022; *Accepted 15 August 2022*; *Published online 16 August 2022*; *Published 1 December 2022*

Abstract
Glycolysis model has been considered by Caputo fractional derivative. We give the topological classifications of fixed points of this model. Then, we show analytically that under certain parametric conditions fractional order glycolysis model underlies a Neimark-Sacker (NS) bifurcation and Flip bifurctaion. By using central manifold and bifurcation theory, we confirm the existence and direction of both NS and Flip bifurcations. To reinforce our analytical findings, we perform numerical simulations that include bifurcations, phase portraits, periodic orbits, invariant closed cycles, abrupt emergence of chaos and abrupt elimination of chaos. At the end, OGY method is applied to eliminate chaotic trajectories of the system.

Keywords fractional order glycolysis model; Flip and Neimark-Sacker (NS) bifurcations; Maximum Lyapunov Exponents (MLEs); Fractal Dimensions (FDs); chaos control.

Network Biology
ISSN 2220-8879
URL: http://www.iaees.org/publications/journals/nb/online-version.asp
RSS: http://www.iaees.org/publications/journals/nb/rss.xml
E-mail: networkbiology@iaees.org
Editor-in-Chief: WenJun Zhang
Publisher: International Academy of Ecology and Environmental Sciences

1 Introduction

Fractional calculus is a 17th century mathematical concept. However, it may be deemed a novel study topic. In fact, the model has fractional derivatives, which has made significant progress in the study of mathematical modeling with memory effect. Fractional-order differential equations can be successfully described in a variety of domains, including science, engineering, finance, economics, and epidemiology (Magin et al,. 2011; Huang et al., 2017, 2018). The order of differentiation in the transition of an integer-order model to a fractional-order model must be precise, and a little modification in order of differentiation α could have a significant impact on the ultimate outcome (Bagley and Calico, 1991). There are numerous techniques when attempting to apply the concept of differentiation to arbitrary order. The most popular definitions are those of Riemann-Liouville, Caputo, and Grünwald-Letnikov (Podlubny, 1999).

In addition to these definitions, several more strategies are being investigated by applied mathematicians. Researchers are looking for the most effective technique including some numerical methods (Jafari and Daftardar-Gejji, 2006; Ameen and Novati, 2017; Momani and Odibat, 2007) while building or modifying their models. The bifurcation of a system in a fractional differential equation has drawn the attention of many scholars, who have thoroughly examined this phenomenon (Elsadany and Matouk, 2015; Balci et al., 2019, 2021; Abdelaziz et al., 2018).

In many discrete systems, the bifurcations (Neimark-Sacker and flip) and stable orbits as well as chaotic attractors attract a great interest, these phenomena can be determined either numerically or by normal form and center manifold theory (Khan and Khalique, 2020; Rana, 2020; Khan et al., 2022).

The metabolic process of converting glucose to pyruvate is known as glycolysis, and during this process, two molecules of pyruvate are normally produced for every molecule of glucose. Glycolysis is a biological activity that occurs in living cells and allows them to obtain energy from glucose and the following differential system can be used to simulate this biological process (Selkov, 1968) and the non-dimensional form of hypothetical glycolysis model is given below.

$$\begin{aligned} \dot{x} &= ay - x + x^2 y \\ \dot{y} &= b - ay - x^2 y \end{aligned} \qquad (1)$$

where x and y are the amounts of adenosine diphosphate (ADP) and fructose-6-phospate (in dimensionless forms), and a and b are kinetics parameter. The requirements for both forms of instabilities are described, and the occurrence of a temporal structure containing limit cycle behavior is numerically determined as a function of the system's essential factors (Goldbeter and Lefever, 1972). The more detailed analysis of glycolysis model was discussed in (Goldbeter and Lefever, 1972; Decroly and Goldbeter, 1982; Wolf et al., 2000; Wei et al., 2015).

The fractional order glycolysis model is given as follows

$$\begin{aligned} D^{\alpha}x(t) &= ay(t) - x(t) + x^2(t)y(t) \\ D^{\alpha}y(t) &= b - ay(t) - x^2(t)y(t) \end{aligned} \qquad (2)$$

where $t > 0$, and α is the fractional order which satisfy $\alpha \in (0, 1]$. There are a lot of approaches for discretizesuch kind of system. One of these is the piecewise constant approximation. The model is discretized by using this method. The process is given as follows:

Let the initial conditions of system (1) are $x(0) = x_0, y(0) = y_0$. The discretized version of system (2) is given as

$$\begin{aligned} D^{\alpha}x(t) &= ay\left(\left[\frac{t}{\rho}\right]\rho\right) - x\left(\left[\frac{t}{\rho}\right]\rho\right) + x^2([\frac{t}{\rho}]\rho)y([\frac{t}{\rho}]\rho) \\ D^{\alpha}y(t) &= b - ay\left(\left[\frac{t}{\rho}\right]\rho\right) - x^2([\frac{t}{\rho}]\rho)y([\frac{t}{\rho}]\rho) \end{aligned} \qquad (3)$$

First, let $t \in [0, \rho)$, so$\frac{t}{\rho} \in [0, 1)$. Thus, we obtain

$$\begin{aligned} D^{\alpha}x(t) &= ay_0 - x_0 + {x_0}^2 y_0 \\ D^{\alpha}y(t) &= b - ay_0 - {x_0}^2 y_0 \end{aligned} \qquad (4)$$

The solution of (4) is reduced to

$$\begin{aligned} x_1(t) &= x_0 + J^{\alpha}(ay_0 - x_0 + {x_0}^2 y_0) = x_0 + \frac{t^{\alpha}}{\alpha\Gamma(\alpha)}(ay_0 - x_0 + {x_0}^2 y_0) \\ y_1(t) &= y_0 + J^{\alpha}(b - ay_0 - {x_0}^2 y_0) = y_0 + \frac{t^{\alpha}}{\alpha\Gamma(\alpha)}(b - ay_0 - {x_0}^2 y_0) \end{aligned} \qquad (5)$$

Second, let $t \in [\rho, 2\rho)$, so $\frac{t}{\rho} \in [1, 2)$. Then

$$D^{\alpha}x(t) = ay_1 - x_1 + {x_1}^2 y_1$$
$$D^{\alpha}y(t) = b - ay_1 - {x_1}^2 y_1 \quad (6)$$

which have the following solution

$$x_2(t) = x_1(\rho) + J_{\rho}^{\alpha}\,(ay_1 - x_1 + {x_1}^2 y_1)$$
$$= x_1(\rho) + \frac{(t-\rho)^{\alpha}}{\alpha\Gamma(\alpha)}(ay_1 - x_1 + {x_1}^2 y_1)$$
$$y_2(t) = y_1(\rho) + J_{\rho}^{\alpha}\,(b - ay_1 - {x_1}^2 y_1)$$
$$= x_1(\rho) + \frac{(t-\rho)^{\alpha}}{\alpha\Gamma(\alpha)}(b - ay_1 - {x_1}^2 y_1) \quad (7)$$

where $J_{\rho}^{\alpha} = \frac{1}{\Gamma(\alpha)}\int_{\rho}^{t}(t-\tau)^{\alpha-1}d\tau, \alpha > 0$. Repeat the discretization process n times, we obtain

$$x_{n+1}(t) = x_n(n\rho) + \frac{(t-n\rho)^{\alpha}}{\alpha\Gamma(\alpha)}\left(ay_n(n\rho) - x_n(n\rho) + {x_n}^2(n\rho)y_n(n\rho)\right)$$

$$y_{n+1}(t) = y_n(n\rho) + \frac{(t-n\rho)^{\alpha}}{\alpha\Gamma(\alpha)}\left(b - ay_n(n\rho) - {x_n}^2(n\rho)y_n(n\rho)\right) \quad (8)$$

where $t \in [n\rho, (n+1)\rho)$. For $t \to (n+1)\rho$, system (8) reduced to

$$x_{n+1} = x_n + \frac{\rho^{\alpha}}{\Gamma(1+\alpha)}(ay_n - x_n + {x_n}^2 y_n)$$

$$y_{n+1} = y_n + \frac{\rho^{\alpha}}{\Gamma(1+\alpha)}(b - ay_n - {x_n}^2 y_n) \quad (9)$$

The remaining part of this paper is organized as follows: The topological divisions of fixed points are examined in Sect. 2. In Sect.3, we demonstrate analytically that the system (9) experiences a Flip or NS bifurcation under a certain parametric condition. In Sect.4, to support our analytical conclusions, we exhibit system dynamics quantitatively, including bifurcation diagrams, phase portraits, MLEs and FDs. In Sect.5, we implement a OGY method to calm the turbulence of the unmanaged system. In Sect.6, we give a succinct discussion.

2 Stability Analysis

The system (9) has a unique fixed point $E(x^*, y^*)$, where $x^* = b$ and $y^* = \frac{b}{a+b^2}$ which always exist for all permissible parameter values.

The Jacobian matrix of system (9) evaluated at $E(x^*, y^*)$ are

$$J(x^*, y^*) = \begin{pmatrix} (1 + (-1 + 2x^*y^*)\frac{\rho^{\alpha}}{\Gamma(1+\alpha)}) & (x^{*2} + a)\frac{\rho^{\alpha}}{\Gamma(1+\alpha)} \\ -2x^*y^*\frac{\rho^{\alpha}}{\Gamma(1+\alpha)} & 1 - (x^{*2} + a)\frac{\rho^{\alpha}}{\Gamma(1+\alpha)} \end{pmatrix} \quad (10)$$

Now the Jacobian matrix at $E(b, \frac{b}{a+b^2})$ is given by

$$J_E = \begin{pmatrix} 1 + \frac{(-a+b^2)}{a+b^2}\frac{\rho^{\alpha}}{\Gamma(1+\alpha)} & (a+b^2)\frac{\rho^{\alpha}}{\Gamma(1+\alpha)} \\ -\frac{2b^2}{a+b^2}\frac{\rho^{\alpha}}{\Gamma(1+\alpha)} & (1 - (a+b^2)\frac{\rho^{\alpha}}{\Gamma(1+\alpha)}) \end{pmatrix} \quad (11)$$

The characteristic polynomial of the Jacobian matrix can be written as

$$F(\lambda) \coloneqq \lambda^2 - Tr(J_E)\lambda + Det(J_E) = 0 \quad (12)$$

where $Tr(J_E)$ is the trace and $Det(J_E)$ is the determinant of the Jacobian matrix J_E, and is given by

$$Tr(J_E) = 2 + \left(-1 - a + b^2(-1 + \frac{2}{a+b^2})\right)\frac{\rho^\alpha}{\Gamma(1+\alpha)}$$

$$Det(J_E) = \frac{a+b^2+(-a^2-2ab^2-a+b^2-b^4)\frac{\rho^\alpha}{\Gamma(1+\alpha)}+(a^2+2ab^2+b^4)\left(\frac{\rho^\alpha}{\Gamma(1+\alpha)}\right)^2}{a+b^2} \quad (13)$$

The eigenvalues of (12) can be written as $\lambda_{1,2} = \frac{Tr(J_E)\pm\sqrt{(Tr(J_E))^2-4Det(J_E)}}{2}$.

Jury Criterion: *The stability condition for the equilibrium point* $E(x^*, y^*)$ *is given as follows* $F(1) > 0, F(-1) > 0, F(0) - 1 < 0$.

Let, $PD_E = \left\{(a,b,\rho,\alpha): \rho = \left(\Gamma(1+\alpha).\frac{A_2\pm\sqrt{L}}{A_1}\right)^{\frac{1}{\alpha}} = \rho_\pm, L \geq 0\right\}$.

where,

$A_1 = a^2 + 2ab^2 + b^4$

$A_2 = a + a^2 - b^2 + 2ab^2 + b^4$

$A_3 = 4a + 4b^2$

$L = {A_2}^2 - A_3 * A_1$

Then the system (9) experience a flip bifurcation at E when parameters (a,b,ρ,α) vary in a small vicinity of PD_E.

Also let

$$NS_E = \left\{(a,b,\rho,\alpha): \rho = \left(\Gamma(1+\alpha).\frac{A_2}{A_1}\right)^{\frac{1}{\alpha}} = \rho_{NS}, L < 0\right\}$$

Then the system (9) experiences a NS bifurcation at E when parameters (a,b,ρ,α) change around the set NS_E.

We give the following Lemma for the stability condition of the fixed point E.

Lemma 1. *For any choice of parameter values, the fixed point E is a*

- *sink if (i)* $L \geq 0, \rho < \rho_-(stable\ node)$,
  (ii) $L < 0, \rho < \rho_{NS}(stable\ focus)$,
- *source (i)* $L \geq 0, \rho < \rho_+(unstable\ node)$,
  (ii) $L < 0, \rho > \rho_{NS}(unstable\ focus)$,
- *non-hyperbolic (i)* $L \geq 0, \rho = \rho_-\ or\ \rho = \rho_+(saddle\ with\ flip)$,
  (ii) $L < 0, \rho = \rho_{NS}(\ focus)$,
- *saddle: otherwise*

3 Bifurcation Analysis

In this section, we will discuss the existence, direction and stability analysis of flip and NS bifurcations near the fixed point E by using center-manifold and bifurcation theory (Kuznetsov, 2013; Wen, 2005; Yao, 2012). We consider ρ as the bifurcation parameter, otherwise stated.

3.1 Flip bifurcation

We choose the parameters (a,b,ρ,α) arbitrarily locate in PD_E. Consider the system (9) at the equilibrium point $E(x^*, y^*)$. Assume the parameters lie in PD_E.

Let, $\rho = \left(\Gamma(1+\alpha).\frac{A_2-\sqrt{L}}{A_1}\right)^{\frac{1}{\alpha}} = \rho_-, L \geq 0$.

And the eigenvalues of J_E are given as

$\lambda_1 = -1$ and $\lambda_2 = 3 + A_2\rho_-$

In order for $|\lambda_2| \neq 1$ implies $A_2\rho_- \neq -2, -4$ (14)

Next, we use the transformation $\hat{x} = x - x^+, \hat{y} = y - y^+$and set $A(\rho_-) = J(x^*, y^*)$. We shift the fixed point of system (9) to the origin. So the system (9) can be written as

$$\begin{pmatrix}\hat{x}\\ \hat{y}\end{pmatrix} \to A(\rho_-)\begin{pmatrix}\hat{x}\\ \hat{y}\end{pmatrix} + \begin{pmatrix}F_1(\hat{x},\hat{y},\rho_-)\\ F_2(\hat{x},\hat{y},\rho_-)\end{pmatrix} \quad (15)$$

where $X = (\hat{x}, \hat{y})^T$ and

$$F_1(\hat{x},\hat{y},\rho_-) = \frac{1}{A_1}\hat{x}^2\hat{y}\left(A_2 - \sqrt{L}\right) + \frac{1}{2}\left[\frac{1}{(a+b^2)^3}2\hat{x}^2 b\left(A_2 - \sqrt{L}\right) + \frac{1}{A_1}4\hat{x}\hat{y}b\left(A_2 - \sqrt{L}\right)\right]$$

$$F_2(\hat{x},\hat{y},\rho_-) = -\frac{1}{A_1}\hat{x}^2\hat{y}\left(A_2 - \sqrt{L}\right) + \frac{1}{2}\left[\frac{-1}{(a+b^2)^3}2\hat{x}^2 b\left(A_2 - \sqrt{L}\right) - \frac{1}{A_1}4\hat{x}\hat{y}b\left(A_2 - \sqrt{L}\right)\right] \quad (16)$$

The system (15) can be expressed as

$$X_{n+1} = AX_n + \frac{1}{2}B(X_n, X_n) + \frac{1}{6}C(X_n, X_n, X_n) + O(\|X_n\|^4)$$

where $B(x,y) = \begin{pmatrix}B_1(x,y)\\ B_2(x,y\end{pmatrix}$ and $C(x,y,v) = \begin{pmatrix}C_1(x,y,v)\\ C_2(x,y,v)\end{pmatrix}$ are symmetric multi-linear vector functions of $x, y, v \in \mathbb{R}^2$ and defined as follows:

$$B_1(x,y) = \sum_{j,k=1}^{2}\frac{\delta^2 F_1(\varepsilon,\rho)}{\delta\varepsilon_j\delta\varepsilon_k}\bigg|_{\varepsilon=0} x_j y_k = \frac{1}{(a+b^2)^3}2b(x_2y_1(a+b^2) + x_1(y_1 + y_2(a+b^2)))\left(A_2 - \sqrt{L}\right)$$

$$B_2(x,y) = \sum_{j,k=1}^{2}\frac{\delta^2 F_2(\varepsilon,\rho)}{\delta\varepsilon_j\delta\varepsilon_k}\bigg|_{\varepsilon=0} x_j y_k = -\frac{1}{(a+b^2)^3}2b(x_2y_1(a+b^2) + x_1(y_1 + y_2(a+b^2)))\left(A_2 - \sqrt{L}\right)$$

and

$$C_1(x,y,v) = \sum_{j,k,l=1}^{2}\frac{\delta^2 F_1(\varepsilon,\rho)}{\delta\varepsilon_j\delta\varepsilon_k\delta\varepsilon_l}\bigg|_{\varepsilon=0} x_j y_k v_l = \frac{1}{(a+b^2)^2}2\left(A_2 - \sqrt{L}\right)(v_2x_1y_1 + v_1x_2y_1 + v_1x_1y_2)$$

$$C_2(x,y,v) = \sum_{j,k,l=1}^{2}\frac{\delta^2 F_1(\varepsilon,\rho)}{\delta\varepsilon_j\delta\varepsilon_k\delta\varepsilon_l}\bigg|_{\varepsilon=0} x_j y_k v_l = -\frac{1}{(a+b^2)^2}2\left(A_2 - \sqrt{L}\right)(v_2x_1y_1 + v_1x_2y_1 + v_1x_1y_2)$$

Let, $q_1, q_2 \in \mathbb{R}^2$ be two eigenvectors of A and A^T for eigenvalue $\lambda_1(\rho_-) = -1$ such that $A(\rho_-)q_1 = -q_1$ and $A^T(\rho_-)q_2 = -q_2$.

Then by direct calculation we get,

$$q_1 = \begin{pmatrix}\dfrac{(A_1(a - a^2 + 3b^2 - 2ab^2 - b^4 + \sqrt{L}))}{(2b^2\left(A_2 - \sqrt{L}\right))}\\ 1\end{pmatrix} = \begin{pmatrix}q_{11}\\ 1\end{pmatrix}$$

$$q_2 = \begin{pmatrix}\dfrac{(A_1(a - a^2 + 3b^2 - 2ab^2 - b^4 + \sqrt{L}))}{(2b^2\left(A_2 - \sqrt{L}\right))}\\ 1\end{pmatrix} = \begin{pmatrix}q_{21}\\ 1\end{pmatrix}$$

In order to get, $< q_1, q_2 > 1$, where $< q_1, q_2 > = q_{11}q_{21} + q_{12}q_{22}$, we have to use the normalized vector $q_2 = \gamma_F q_2$, with $\gamma_F = \frac{1}{1+q_{11}q_{21}}$.

To obtain the direction of the flip bifurcation, we have to check the sign of $l_1(\rho_-)$, the coefficient of critical normal form (Kuzenetsov, 1998) and is given by

$$l_1(\rho_-) = \frac{1}{6} < q_2, C(q_1, q_1, q_1) > -\frac{1}{2} < q_2, B(q_2, (A-I)^{-1}B(q_1, q_1)) > \quad (17)$$

According to above discussion, the direction and stability of Flip bifurcation can be presented in the following theorem

Theorem 1. *Suppose (14) holds and* $l_1(\rho_-) \neq 0$, *then Flip bifurcation at fixed point* $E(x^*, y^*)$ *for system (9)*

if the ρ *changes its value in small neighbourhood of* PD_E. *Moreover, if* $l_1(\rho_-) < 0$ *(resp.* $l_1(\rho_-) > 0$*), then*

there exists attracting (resp. repelling) smooth closed invariant curve bifurcate from $E(x^*, y^*)$ *and the bifurcationis sub-critical (resp. super-critical).*

3.2 Neimark-Sacker bifurcation

When $L < 0$ and the parameters $(a, b, \rho, \alpha) \in NS_E$, then the eigenvalues of system (12) are given by

$$\lambda, \bar{\lambda} = \frac{Tr(J_E) \pm \sqrt{4Det(J_E) - Tr(J_E)^2}}{2} \quad (18)$$

Let, $\rho = \rho_{NS} = \left(\Gamma(1+\alpha).\frac{A_2}{A_1}\right)^{\frac{1}{\alpha}}$

Moreover, the transversality and non-resonance conditions yield

$$\frac{d|\lambda_i(\rho)|}{d\rho}\Big|_{\rho=\rho_{NS}} = \frac{2A_2}{A_3} \neq 0$$

$$-(Tr(J_E))|_{\rho=\rho_{NS}} \neq 0 \Rightarrow \frac{4A_2^2}{A_1 A_3} \neq 2,3 \quad (19)$$

Using the transformation $\hat{x} = x - x^+, \hat{y} = y - y^+$and set $A(\rho) = J(x^*, y^*)$. We shift the fixed point of system (9) to the origin. So the system (9) can be written as

$$X = A(\rho)X + F \quad (20)$$

where $X = (\hat{x}, \hat{y})^T$ and $F = (F_1, F_2)^T$ are given by

$$F_1(\hat{x}, \hat{y}, \rho_{NS}) = \frac{A_2}{A_1}\hat{x}^2\hat{y} + \frac{1}{2}\left[\frac{1}{(a+b^2)^3}2\hat{x}^2 b(A_2) + \frac{1}{A_1}4\hat{x}\hat{y}b(A_2)\right]$$

$$F_2(\hat{x}, \hat{y}, \rho_{NS}) = -\frac{A_2}{A_1}\hat{x}^2\hat{y} - \frac{1}{2}\left[\frac{1}{(a+b^2)^3}2\hat{x}^2 b(A_2) + \frac{1}{A_1}4\hat{x}\hat{y}b(A_2)\right] \quad (21)$$

The system (20) can be expressed as

$$X_{n+1} = AX_n + \frac{1}{2}B(X_n, X_n) + \frac{1}{6}C(X_n, X_n, X_n) + O(\|X_n\|^4)$$

where $B(x, y) = \begin{pmatrix} B_1(x, y) \\ B_2(x, y \end{pmatrix}$ and $C(x, y, v) = \begin{pmatrix} C_1(x, y, v) \\ C_2(x, y, v) \end{pmatrix}$ are symmetric multi-linear vector functions of $x, y, v \in \mathbb{R}^2$ and defined as follows:

$$B_1(x, y) = \sum_{j,k=1}^{2} \frac{\delta^2 F_1(\varepsilon, \rho)}{\delta\varepsilon_j \delta\varepsilon_k}\Big|_{\varepsilon=0} x_j y_k = \frac{1}{(a+b^2)^3}2b(x_2 y_1(a+b^2) + x_1(y_1 + y_2(a+b^2)))(A_2)$$

$$B_2(x, y) = \sum_{j,k=1}^{2} \frac{\delta^2 F_2(\varepsilon, \rho)}{\delta\varepsilon_j \delta\varepsilon_k}\Big|_{\varepsilon=0} x_j y_k = -\frac{1}{(a+b^2)^3}2b(x_2 y_1(a+b^2) + x_1(y_1 + y_2(a+b^2)))(A_2)$$

and

$$C_1(x,y,v)=\sum_{j,k,l=1}^{2}\frac{\delta^2F_1(\varepsilon,\rho)}{\delta\varepsilon_j\delta\varepsilon_k\delta\varepsilon_l}\bigg|_{\varepsilon=0}x_jy_kv_l=\frac{1}{(a+b^2)^2}2(A_2)(v_2x_1y_1+v_1x_2y_1+v_1x_1y_2)$$

$$C_2(x,y,v)=\sum_{j,k,l=1}^{2}\frac{\delta^2F_1(\varepsilon,\rho)}{\delta\varepsilon_j\delta\varepsilon_k\delta\varepsilon_l}\bigg|_{\varepsilon=0}x_jy_kv_l=-\frac{1}{(a+b^2)^2}2(A_2)(v_2x_1y_1+v_1x_2y_1+v_1x_1y_2)$$

Suppose, $q_1,q_2\in\mathbb{C}^2$ be two eigenvectors of A and A^T for eigenvalue $\lambda(\rho_{NS})$, $\overline{\lambda}(\rho_{NS})$ such that

$$A(\rho_{NS})q_1=\lambda(\rho_{NS})q_1, A(\rho_{NS})\overline{q_1}=\bar{\lambda}(\rho_{NS})\overline{q_1}$$

$$A^T(\rho_{NS})q_2=\bar{\lambda}(\rho_{NS})q_2,\ A^T(\rho_{NS})\overline{q_2}=\lambda(\rho_{NS})\overline{q_2} \quad (22)$$

Then by direct calculation, we get

$$q_1=\begin{pmatrix}-\dfrac{a^2+b^2+b^4+a(-1+2b^2)-\sqrt{L}}{4b^2}\\1\end{pmatrix}=\begin{pmatrix}\eta_1+i\eta_2\\1\end{pmatrix}$$

where $\eta_1=$-$\frac{a^2+b^2+b^4+a(-1+2b^2)}{4b^2}$; $\eta_2=\frac{-\sqrt{-L}}{4b^2}$

$$q_2=\begin{pmatrix}\dfrac{a^2+b^2+b^4+a(-1+2b^2)+\sqrt{L}}{2A_1}\\1\end{pmatrix}=\begin{pmatrix}\vartheta_1+i\vartheta_2\\1\end{pmatrix}$$

where $\vartheta_1=\frac{a^2+b^2+b^4+a(-1+2b^2)}{2A_1}$; $\vartheta_2=\frac{-\sqrt{-L}}{2A_1}$

For $<q_1,q_2>1$, where $<q_1,q_2>=q_{11}q_{21}+q_{12}q_{22}$,we have to use the normalized vector $q_2=\gamma_{Ns}q_2$, with $\gamma_{NS}=\frac{1}{1-(\vartheta_1+i\vartheta_2)(\eta_1-i\eta_2)}$.

So the eigenvectors are computed as follows:

$$q_1=\begin{pmatrix}\eta_1+i\eta_2\\1\end{pmatrix}$$

$$q_2=\begin{pmatrix}\dfrac{\vartheta_1+i\vartheta_2}{1-(\vartheta_1+i\vartheta_2)(\eta_1-i\eta_2)}\\\dfrac{1}{1-(\vartheta_1+i\vartheta_2)(\eta_1-i\eta_2)}\end{pmatrix}$$

We decompose $X\in\mathbb{R}^2$ as $X=zq_1+\overline{zq_1}$ by considering ρ vary near to ρ_{NS} and for $z\in\mathbb{C}$. The explicit formula of z is $z=\langle q_2,X\rangle$. So, the system (9) transformed to the following system for $|\rho|$ close to ρ_{NS}:

$$z\to\lambda(\rho)z+\hat{g}(z,\bar{z},\rho) \quad (23)$$

where $\lambda(\rho)=(1+\varphi(\rho))e^{i\theta\rho}$ with $\varphi(\rho_{NS})=0$ and $\hat{g}(z,\bar{z},\rho)$is a smooth complex-valued function.

After Taylor expression of g with respect to $(z,\bar{z})$, we obtain

$\hat{g}(z,\bar{z},\rho)=\sum_{k+l\geq2}\frac{1}{k!l!}\widehat{g_{kl}}(\rho)z^kz^{-l}$, with $\widehat{g_{kl}}\in\mathbb{C},k,l=0,1,\ldots$

According to multilinear symmetric vector functions, the coefficients g_{kl} are

$\widehat{g_{20}}(\rho_{NS})=\langle q_2,B(q_1,q_1)\rangle,\widehat{g_{11}}(\rho_{NS})=\langle q_2,B(q_1,\overline{q_1})\rangle$

$$\widehat{g_{02}}(\rho_{NS}) = \langle q_2, B(\overline{q_1}, \overline{q_1})\rangle, \widehat{g_{21}}(\rho_{NS}) = \langle q_2, C(q_1, q_1, \overline{q_1})\rangle \quad (24)$$

The sign of first Lyapunov coefficient $l_2(\rho_{NS})$ determines the direction of NS bifurcation and is defined by

$$l_2(\rho_{NS}) = Re\left(\frac{\lambda_2 \widehat{g_{21}}}{2}\right) - Re\left(\frac{(1-2\lambda_1)\lambda_2{}^2 \widehat{g_{20}}\widehat{g_{11}}}{2(1-\lambda_1)}\right) - \frac{1}{2}|\widehat{g_{11}}|^2 - \frac{1}{2}|\widehat{g_{02}}|^2 \quad (25)$$

We give the following theorem regarding the direction and stability of the Neimark-Sacker bifurcation in light of the aforementioned study.

Theorem 2. *Suppose (19) holds and* $l_2(\rho_{NS}) \neq 0$, *then NS bifurcation at fixed point* $E(x^*, y^*)$ *for system (9)*

if the ρ *changes its value in small neighbourhood of* NS_E. *Moreover, if* $l_2(\rho_{NS}) < 0$ *(resp.* $l_2(\rho_{NS}) > 0$*), then there exists attracting (resp. repelling) smooth closed invariant curve bifurcate from* $E(x^*, y^*)$ *and the bifurcation is sub-critical (resp. super-critical).*

4 Numerical Simulations

We will use numerical simulations to support our theoretical conclusions for system (9) in this part, which will include diagrams of bifurcation, phase portraits, MLEs and FDs.

Example 1: We choose the values of the parameters as $a = 2.05, b = 1.61, \alpha = 0.5896$ and , ρ varies in the range $0.38 \leq \rho \leq 0.78$. We find a fixed point $E(x^*, y^*) = (1.61, 0.346826)$ and the bifurcation point for the system (9) is $\rho_F = 0.4255$. The eigenvalues are $\lambda_{1,2} = -1, -0.0641301$. The corresponding eigenvectors are

$q_1 \sim (-0.834056, 0.551679)^T$ and $q_2 \sim (0.341808, 0.93977)^T$

For $< q_1, q_2 > = 1$, then we can take the normalized factor $\gamma_F = 4.28515$.

From (17), we get $l_1(\rho_-) = 0.579167 > 0$. Therefore, the Flip bifurcation is sub-critical and the requirements of Theorem 1 is fulfilled.

We can observe from Fig. 1(a-b) that fixed point stability occurs for $\rho < \rho_F$, loses its stability at $\rho = \rho_F$, and a period doubling phenomenon leads to chaos for $\rho > \rho_F$. Fig. 1(c-d) shown MLEs and FD related to Fig. 1(a-b). We note the occurrence of the period -2, -4, -8, and -16 orbits and chaotic set for different values of ρ. The status of stable, periodic, or chaotic dynamics are compatible with sign in Fig. 1 (c-d), as defined by the Maximum Lyapunov Exponent. The phase portrait of bifurcations diagrams corresponding to Fig. 1 for different values of $\rho \in [0.38, 0.78]$ depicted in Fig. 2.

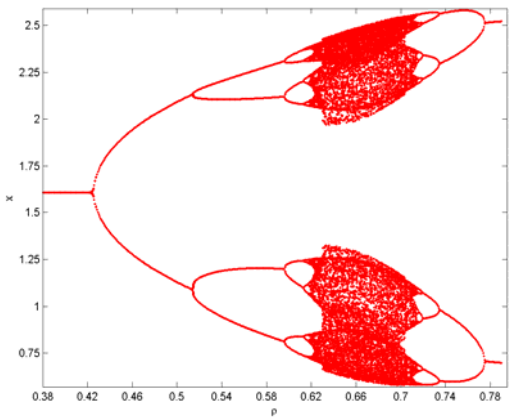

(a)

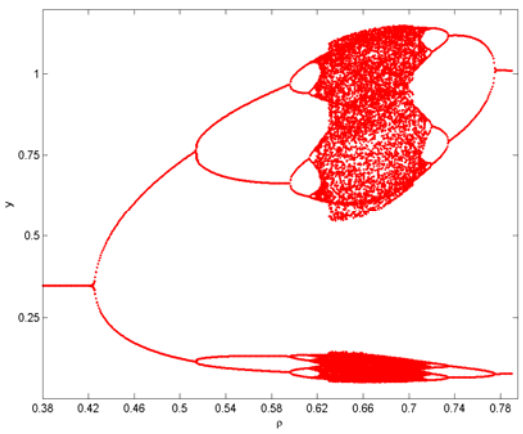

(b)

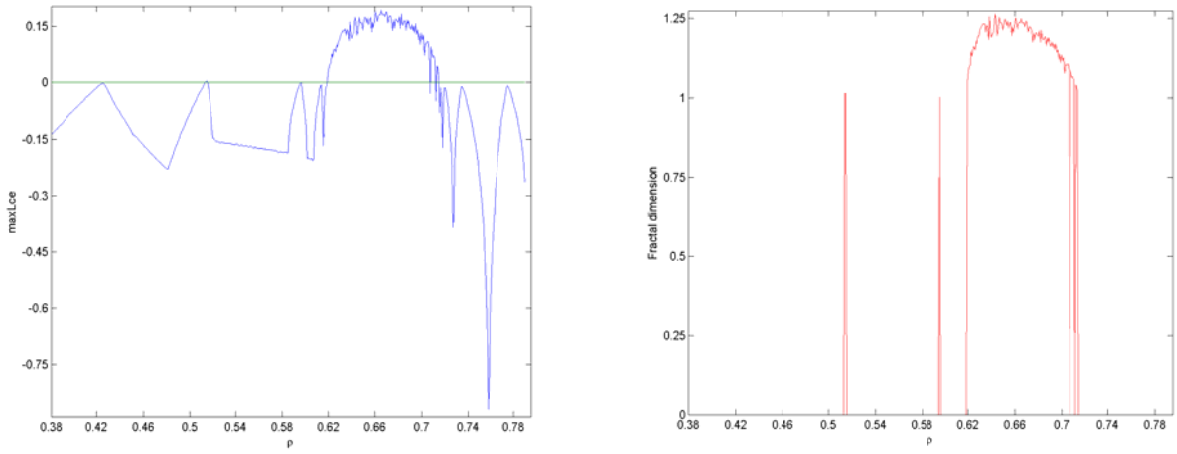

(c) (d)

Fig. 1 Flip Bifurcation diagram with $a = 2.05, b = 1.61, \alpha = 0.4255, \rho \in [0.38, 0.78]$ $(x_0, y_0) = (1.61, 0.346826)$ in (a) (ρ, x) plane (b) (ρ, y) plane (c,d) MLEs and FD.

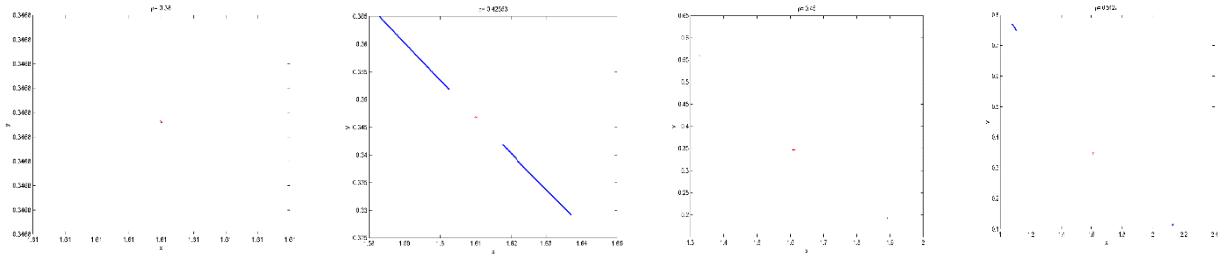

(a) (b) (c) (d)

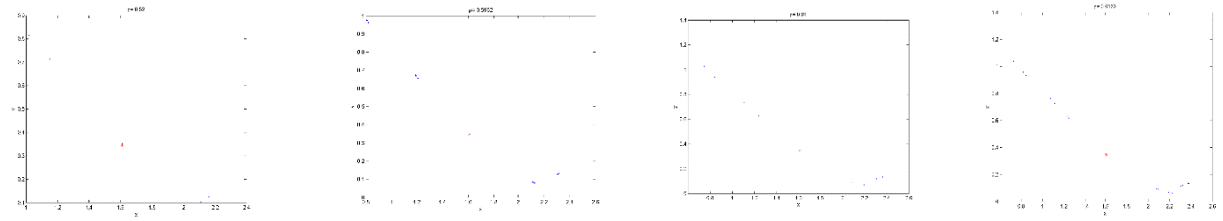

(e) (f) (g) (h)

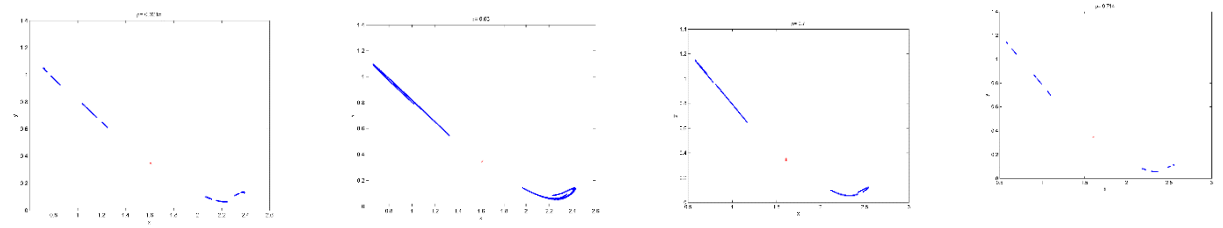

(i) (j) (k) (l)

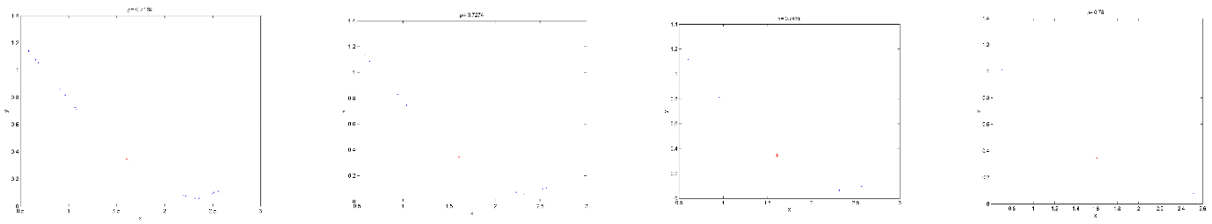

(m) (n) (o) (p)

Fig. 2 Phase portrait for different values of ρ corresponding to Fig. 1. Red * indicates the fixed point.

Example 2: We choose the values of the parameters as $a = 0.2, b = 0.9, \alpha = 0.5896$ and $, \rho$ varies in the range $0.13 \leq \rho \leq 0.378$. We see an NS bifurcation at the fixed point $E(x^*, y^*) = (0.9, 0.891089)$ and the critical value of the bifurcation point for the system (9) is $\rho_{NS} = 0.1758$. The eigenvalues are $\lambda, \bar{\lambda} = 0.91837 \pm 0.395752i$.

And,

$$\frac{d|\lambda_i(\rho)|}{d\rho}\Big|_{\rho=\rho_{NS}} = \frac{2A_2}{A_3} = 0.20302 \neq 0$$

$$-(Tr(J_E))|_{\rho=\rho_{NS}} \neq 0 \Rightarrow \frac{4A_2^2}{A_1 A_3} = 0.163236 \neq 2{,}3$$

The corresponding eigenvectors are

$q_1 \sim (-0.394109 - 0.480692i, 0.783335)^T$ and $q_2 \sim (0.78335, -0.394109 + 0.480692i)^T$

For $< q_1, q_2 > = 1$, then we can take the normalized factor $\gamma_{NS} = -0.132787i$.

Also,

$$\widehat{g_{20}} = 0.461251 - 0.0844134i$$
$$\widehat{g_{11}} = 0.108504 - 0.0878579i$$
$$\widehat{g_{02}} = 0.178502 - 0.433607i$$
$$\widehat{g_{21}} = -0.390766 - 0.277891i$$

From(25) we get $l_2(\rho_{NS}) = -0.215105 < 0$. Therefore, the NS bifurcation is super-critical and the requirements of Theorem 2 are fulfilled.

We can observe from the bifurcation diagrams in Fig. 3(a-b) that fixed point stability occurs for $\rho < \rho_{NS}$, loses its stability at $\rho = \rho_{NS}$, and an attracting invariant curve appears for $\rho > \rho_{NS}$. The MLEs and FD shown in Fig 3(c-d) corresponding to Fig. 3(a-b), which substantiate the existence of chaos and the period-10, -11, and -22 as ρ varies. The phase portrait of bifurcation diagrams corresponding to Fig. 3 for different values of $\rho \in [0.13,0.37]$ depicted in Fig. 4, which demonstrates the smooth invariant curve's behavior in detail, showing how it splits from the stable fixed point and grows in radius.

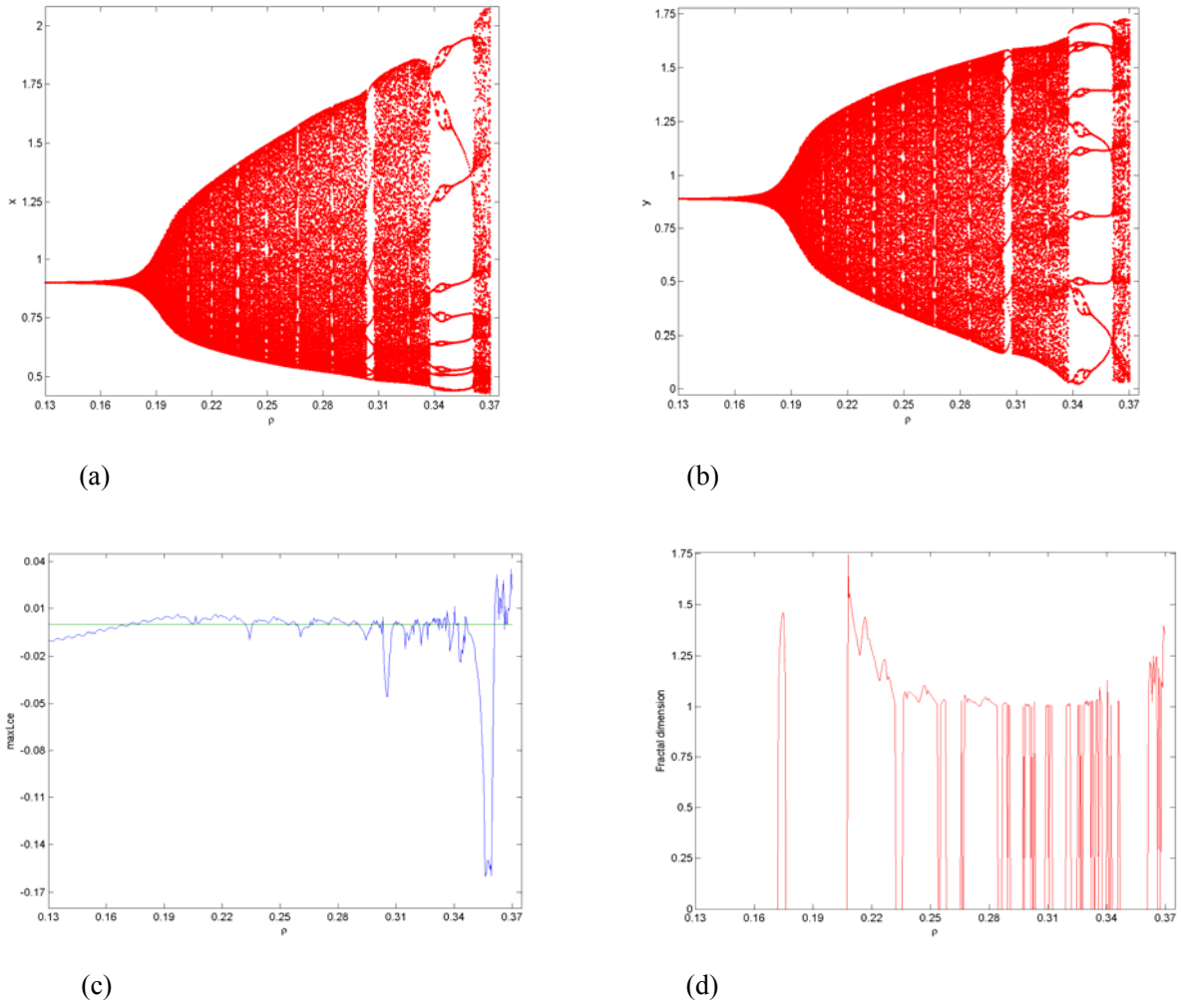

Fig. 3 NS Bifurcation diagram with $\alpha = 0.2, b = 0.9, \alpha = 0.5896, \rho \in [0.13,0.37\,]\,(x_0, y_0) = (0.9,0.891)$ in (a) (ρ, x) plane (b) (ρ, y) plane (c,d) MLEs and FD.

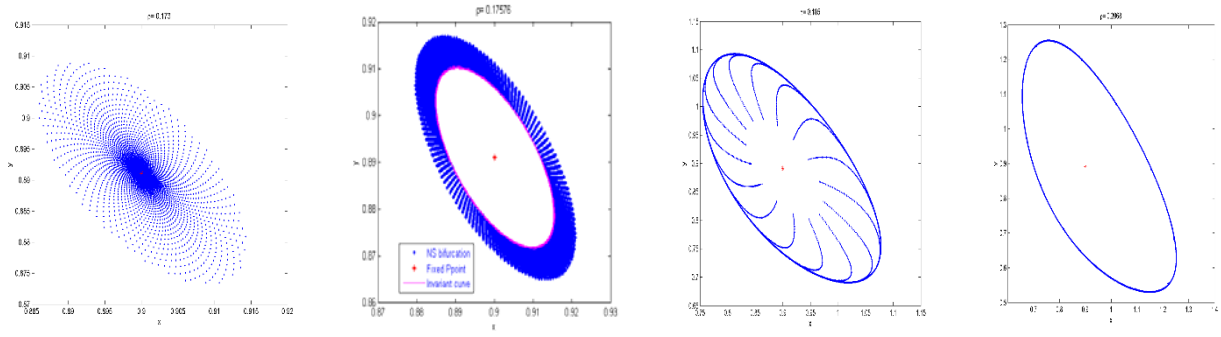

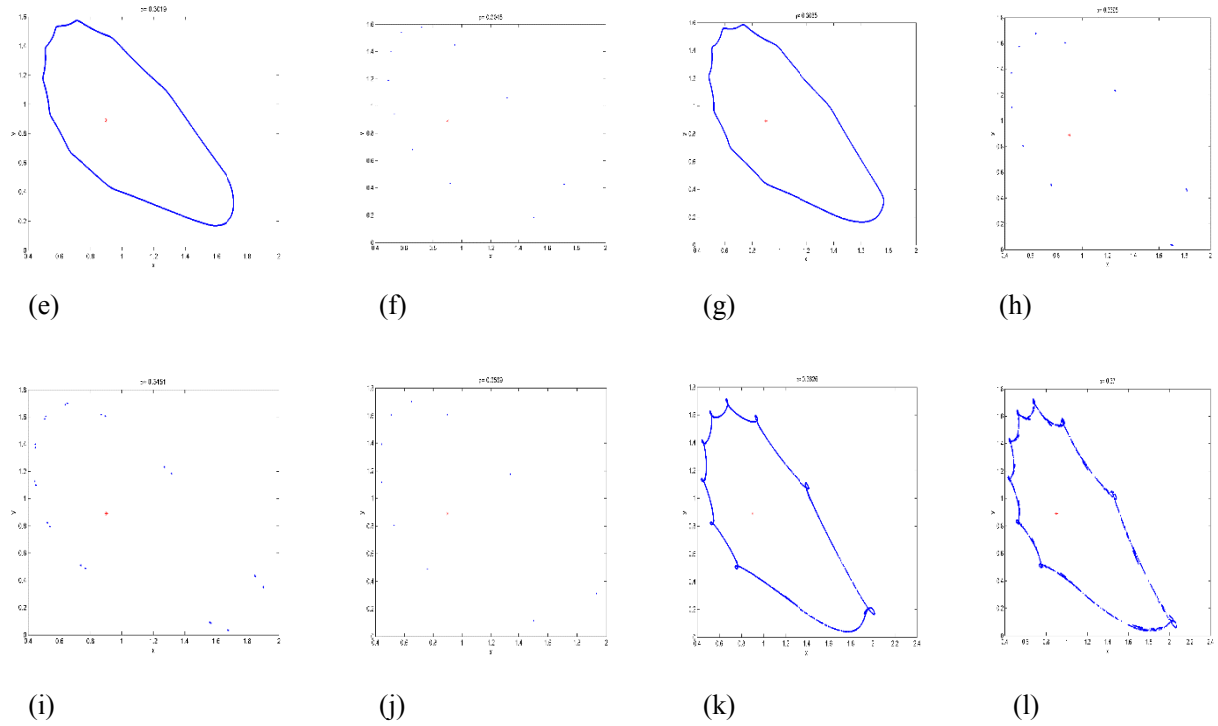

(e) (f) (g) (h)

(i) (j) (k) (l)

Fig. 4 Phase portrait for different values of ρ corresponding to Fig. (7). Red * indicates the fixed point.

Example 3: The Neimark-Sacker bifurcation diagram may show more dynamical behaviour for the glycolysis system as other parameter values vary (e.g. parameter a). A new Neimark-Sacker bifurcation diagram is created as shown in Fig. 5(a-b) when the parameter values are set as in Example 2 with $\rho = 0.1758$ and a ranging between $0.02 \leq a \leq 0.3$. At $a = a_{NS}$~0.0808, a Neimark-Sacker bifurcation occurs in the system.It is calculated and presented in Fig. 5(c) that the maximum Lyapunov exponent that corresponds to Fig. 5(a-b) which confirms the existence of chaos and the period window as varying parameter$a$.The smooth invariant curve's behavior is demonstrated in detail in the phase portrait of bifurcation diagrams for various values of a in Fig. 6. This figure shows how the smooth invariant curve splits from the stable fixed point and increases in radius. Additionally, periodic windows with attracting chaotic sets and periods of -17 and -34 are discovered on the route to chaos.

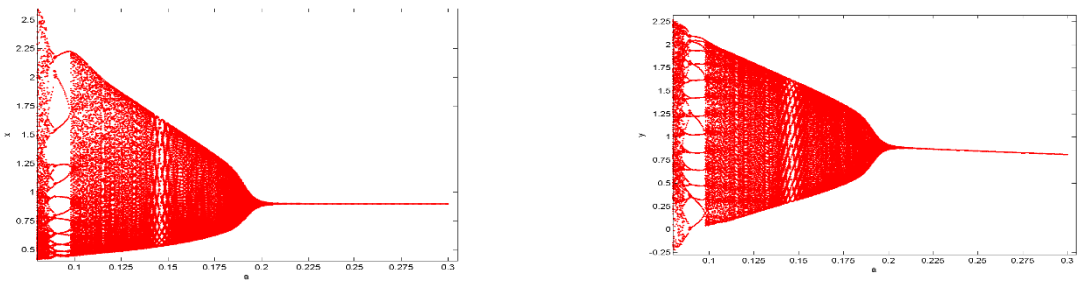

(a) (b)

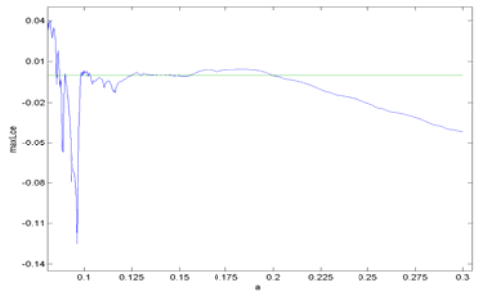

(c)

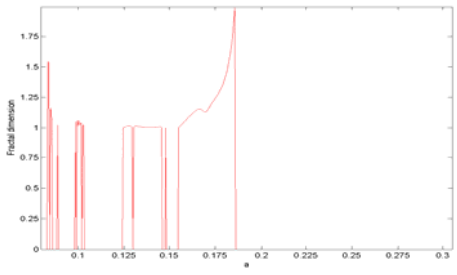

(d)

Fig. 5 NS Bifurcation diagram with $b = 0.9, \alpha = 0.5896, \rho = 0.1758,\ a \in [0.02,0.3]$ $(x_0, y_0) = (0.9,0.891)$ in (a) (a, x) plane (b) (a, y) plane (c,d) MLEs and FD.

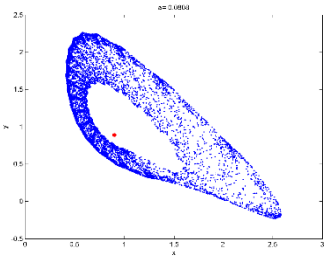

(a)

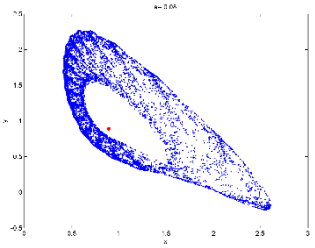

(b)

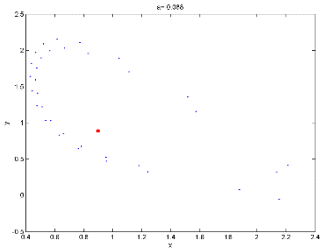

(c)

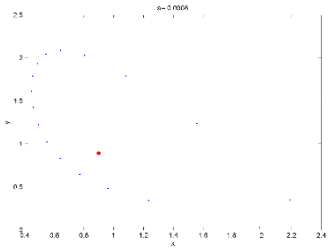

(d)

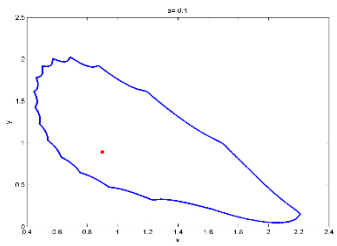

(e)

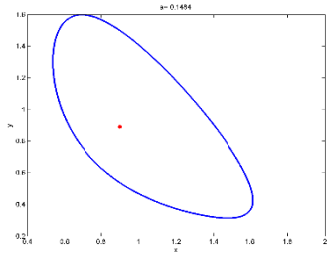

(f)

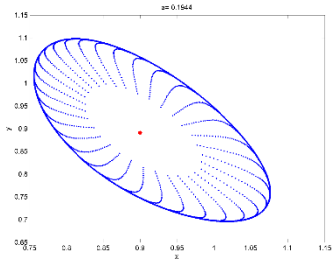

(g)

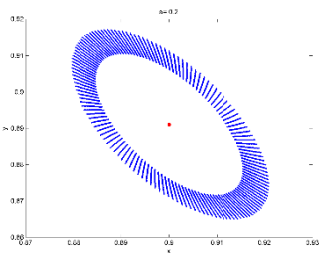

(h)

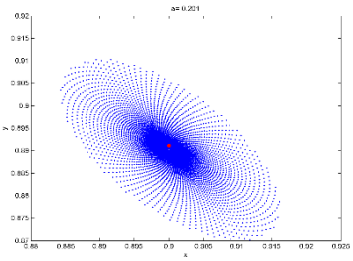

(i)

Fig. 6 Phase portrait for different values of a corresponding to Fig. 5. The fixed point is marked with a red *.

A system's chaotic attractors are identified by the fractal dimensions (FD), which are defined in (Cartwright, 1999):

$$\ddot{F}_L = k + \frac{\sum_{j=1}^{k} s_j}{|s_{j+1}|}$$

where k is the largest integer such that $\sum_{j=1}^{k} s_j \geq 0$ and $\sum_{j=1}^{k+1} s_j < 0$ and s_j's are Lyapunov exponents. The fractal dimensions now have the form for the system (9):

$$\ddot{F}_L = 2 + \frac{s_1 + s_2}{|s_3|}$$

Increasing the value of the parameter ρ results in an unstable system dynamics for the fractional order glycolysis model because the chaotic dynamics of the system (9) (see Fig. 4) are quantized with the sign of the FD (see Fig. 3(d)).

5 Chaos Control

Controlling chaos is a challenging issue. For controlling chaos in fractional order glycolysis model we introduce OGY control strategy, taking a as a control parameter. We reformat system (9) as follows in order to use the OGY approach first described by Edward et al. (1990):

$$x_{n+1} = x_n + \frac{\rho^\alpha}{\Gamma(1+\alpha)}(ay_n - x_n + {x_n}^2 y_n) = \widetilde{z_1}(x, y, a)$$
$$y_{n+1} = y_n + \frac{\rho^\alpha}{\Gamma(1+\alpha)}(b - ay_n - {x_n}^2 y_n) = \widetilde{z_2}(x, y, a) \qquad (26)$$

where a stands for a parameter used to regulate chaos. Additionally, a is constrained to exist in a certain narrow interval $|a - a_0| < \vartheta$ with $\vartheta > 0$ and a_0 denotes the nominal value associated with the chaotic zone. To direct the trajectory towards the intended orbit, we use the stabilizing feedback control approach. Consider the possibility that the system's (9) unstable fixed point (x^+, y^+) is located in an area of chaos brought on by the appearance of a Neimark-Sacker bifurcation, then the system (29) can be approximated by the following linear map in the vicinity of the unstable fixed point (x^+, y^+):

$$\begin{bmatrix} x_{n+1} - x^+ \\ y_{n+1} - y^+ \end{bmatrix} \approx \tilde{A} \begin{bmatrix} x_n - x^+ \\ y_n - y^+ \end{bmatrix} + \tilde{B}[a - a_0]$$

where,
$$\tilde{A} = \begin{bmatrix} \frac{\partial \widetilde{z_1}(x,y,a)}{\partial x} & \frac{\partial \widetilde{z_1}(x,y,a)}{\partial y} \\ \frac{\partial \widetilde{z_2}(x,y,a)}{\partial x} & \frac{\partial \widetilde{z_2}(x,y,a)}{\partial y} \end{bmatrix} = \begin{bmatrix} 1 + \frac{(-a+b^2)\frac{\rho^\alpha}{\Gamma(1+\alpha)}}{a+b^2} & (a+b^2)\frac{\rho^\alpha}{\Gamma(1+\alpha)} \\ \frac{-2b^2\frac{\rho^\alpha}{\Gamma(1+\alpha)}}{a+b^2} & 1 - (a+b^2)\frac{\rho^\alpha}{\Gamma(1+\alpha)} \end{bmatrix}$$

and

$$\tilde{B} = \begin{bmatrix} \frac{\partial \widetilde{z_1}(x,y,a)}{\partial a} \\ \frac{\partial \widetilde{z_2}(x,y,a)}{\partial a} \end{bmatrix} = \begin{bmatrix} b\frac{\rho^\alpha}{\Gamma(1+\alpha)} \\ a+b^2 \\ -b\frac{\rho^\alpha}{\Gamma(1+\alpha)} \\ a+b^2 \end{bmatrix}$$

The subsequent matrix is calculated to determine if the system (26) is controllable:

$$\tilde{C} = [\tilde{B} : \tilde{A}\tilde{B}] = \begin{bmatrix} \frac{b\frac{\rho^\alpha}{\Gamma(1+\alpha)}}{a+b^2} & b\frac{\rho^\alpha}{\Gamma(1+\alpha)}\left(-\frac{\rho^\alpha}{\Gamma(1+\alpha)} + \frac{a - a\frac{\rho^\alpha}{\Gamma(1+\alpha)} + b^2\left(1+\frac{\rho^\alpha}{\Gamma(1+\alpha)}\right)}{(a+b^2)^2}\right) \\ \frac{-2b\frac{\rho^\alpha}{\Gamma(1+\alpha)}}{a+b^2} & \frac{b\frac{\rho^\alpha}{\Gamma(1+\alpha)}\left(a^2\frac{\rho^\alpha}{\Gamma(1+\alpha)} + a\left(-1+2b^2\frac{\rho^\alpha}{\Gamma(1+\alpha)}\right) + b^2\left(-1+(-2+b^2)\frac{\rho^\alpha}{\Gamma(1+\alpha)}\right)\right)}{(a+b^2)^2} \end{bmatrix}.$$

At positive fixed point, $\tilde{C}$ has rank 2. Assume that $[a - a_0] = -\widetilde{K}\begin{bmatrix} x_n - x^+ \\ y_n - y^+ \end{bmatrix}$, where $\widetilde{K} = [\ddot{\sigma}_1 \quad \ddot{\sigma}_2]$, then

system (26) can be written as $\begin{bmatrix} x_{n+1}-x^+ \\ y_{n+1}-y^+ \end{bmatrix} \approx [\tilde{A}-\tilde{B}\tilde{K}] \begin{bmatrix} x_n-x^+ \\ y_n-y^+ \end{bmatrix}$

The appropriate controlled system of (9) is also provided by

$$x_{n+1} = x_n + \frac{\rho^\alpha}{\Gamma(1+\alpha)}((a_0 - \ddot{\sigma}_1(x_n - x^+) - \ddot{\sigma}_2(y_n - y^+))y_n - x_n + {x_n}^2 y_n)$$

$$y_{n+1} = y_n + \frac{\rho^\alpha}{\Gamma(1+\alpha)}(b - (a_0 - \ddot{\sigma}_1(x_n - x^+) - \ddot{\sigma}_2(y_n - y^+))y_n - {x_n}^2 y_n) \quad (27)$$

Furthermore, the system's fixed point (x^+, y^+) is locally asymptotically stable if the modulus of the matrix's $(\tilde{A}-\tilde{B}\tilde{K})$ eigenvalues is smaller than 1. The regulated system's (27) Jacobian matrix $(\tilde{A}-\tilde{B}\tilde{K})$ can be expressed as follows:

$$\tilde{A}-\tilde{B}\tilde{K} = \begin{bmatrix} 1+\left(-1+\frac{2b^2}{a+b^2}\right)\frac{\rho^\alpha}{\Gamma(1+\alpha)} - \frac{b\frac{\rho^\alpha}{\Gamma(1+\alpha)}\ddot{\sigma}_1}{a+b^2} & (a+b^2)\frac{\rho^\alpha}{\Gamma(1+\alpha)} - \frac{b\frac{\rho^\alpha}{\Gamma(1+\alpha)}\ddot{\sigma}_2}{a+b^2} \\ -\frac{2b^2\frac{\rho^\alpha}{\Gamma(1+\alpha)}}{a+b^2} + \frac{b\frac{\rho^\alpha}{\Gamma(1+\alpha)}\ddot{\sigma}_1}{a+b^2} & 1+(-a-b^2)\frac{\rho^\alpha}{\Gamma(1+\alpha)} + \frac{b\frac{\rho^\alpha}{\Gamma(1+\alpha)}\ddot{\sigma}_2}{a+b^2} \end{bmatrix}$$

The characteristic equation of the Jacobian matrix $\tilde{A}-\tilde{B}\tilde{K}$ is given by

$$\ddot{\lambda}^2 - \left(2+(-a-b^2)\frac{\rho^\alpha}{\Gamma(1+\alpha)} + \left(-1+\frac{2b^2}{a+b^2}\right)\frac{\rho^\alpha}{\Gamma(1+\alpha)} - \frac{b\frac{\rho^\alpha}{\Gamma(1+\alpha)}\ddot{\sigma}_1}{a+b^2} + \frac{b\frac{\rho^\alpha}{\Gamma(1+\alpha)}\ddot{\sigma}_2}{a+b^2}\right)\ddot{\lambda} + \frac{1}{a+b^2}\Big(a+b^2-(a+a^2-$$

$$b^2+2ab^2+b^4)\frac{\rho^\alpha}{\Gamma(1+\alpha)} + (a^2+2ab^2+b^4)\left(\frac{\rho^\alpha}{\Gamma(1+\alpha)}\right)^2 - b\frac{\rho^\alpha}{\Gamma(1+\alpha)}\ddot{\sigma}_1 - b\left(-1+\frac{\rho^\alpha}{\Gamma(1+\alpha)}\right)\frac{\rho^\alpha}{\Gamma(1+\alpha)}\ddot{\sigma}_2\Big) = 0 \quad (28)$$

Assume $\ddot{\lambda}_1$ and $\ddot{\lambda}_2$ be the roots of the equation (28), then

$$\ddot{\lambda}_1 + \ddot{\lambda}_2 = 2+(-a-b^2)\frac{\rho^\alpha}{\Gamma(1+\alpha)} + \left(-1+\frac{2b^2}{a+b^2}\right)\frac{\rho^\alpha}{\Gamma(1+\alpha)} - \frac{b\frac{\rho^\alpha}{\Gamma(1+\alpha)}\ddot{\sigma}_1}{a+b^2} + \frac{b\frac{\rho^\alpha}{\Gamma(1+\alpha)}\ddot{\sigma}_2}{a+b^2} \quad (29)$$

$$\ddot{\lambda}_1\ddot{\lambda}_2 = \frac{1}{a+b^2}\left(a+b^2-(a+a^2-b^2+2ab^2+b^4)\frac{\rho^\alpha}{\Gamma(1+\alpha)} + (a^2+2ab^2+b^4)\left(\frac{\rho^\alpha}{\Gamma(1+\alpha)}\right)^2 - b\frac{\rho^\alpha}{\Gamma(1+\alpha)}\ddot{\sigma}_1 - b\left(-1+\frac{\rho^\alpha}{\Gamma(1+\alpha)}\right)\frac{\rho^\alpha}{\Gamma(1+\alpha)}\ddot{\sigma}_2\right) \quad (30)$$

The lines of minimal stability for the appropriate controlled system are then obtained by taking $\ddot{\lambda}_1 = \pm 1$ and $\ddot{\lambda}_1\ddot{\lambda}_2 = 1$. Additionally, these limitations guarantee that $\ddot{\lambda}_1$ and $\ddot{\lambda}_2$ are inside the open unit disk. Consider that $\ddot{\lambda}_1\ddot{\lambda}_2 = 1$, then (30) gives

$$\ddot{K}_1 = \frac{1}{a+b^2}\frac{\rho^\alpha}{\Gamma(1+\alpha)}\left(-(a+a^2-b^2+2ab^2+b^4) + (a^2+2ab^2+b^4)\frac{\rho^\alpha}{\Gamma(1+\alpha)} - b\ddot{\sigma}_1 - \left(b-b\frac{\rho^\alpha}{\Gamma(1+\alpha)}\right)\ddot{\sigma}_2\right)$$

Using the assumption that $\ddot{\lambda}_1 = 1$, (29) and (30) result in:

$$\ddot{K}_2 = \frac{1}{a+b^2}\Big(4a+4b^2-(2a+2a^2-2b^2+4ab^2+2b^4)\frac{\rho^\alpha}{\Gamma(1+\alpha)} + (a^2+2ab^2+b^4)\left(\frac{\rho^\alpha}{\Gamma(1+\alpha)}\right)^2 - 2b\frac{\rho^\alpha}{\Gamma(1+\alpha)}\ddot{\sigma}_1 - b\left(-2+\frac{\rho^\alpha}{\Gamma(1+\alpha)}\right)\frac{\rho^\alpha}{\Gamma(1+\alpha)}\ddot{\sigma}_2\Big)$$

Taking $\ddot{\lambda}_1 = -1$ as the final step, we have from Eqs. (29) and (30)

$$\ddot{K}_3 = -\frac{\left(\frac{\rho^\alpha}{\Gamma(1+\alpha)}\right)^2((a+b^2)^2 - b\ddot{\sigma}_2)}{a+b^2}$$

Then, for specific parametric values, stable eigenvalues are found in the triangle in the $\ddot{\sigma}_1\ddot{\sigma}_2 -$ plane enclosed by the straight lines $\ddot{K}_1, \ddot{K}_2$ and $\ddot{K}_3$.

Example 4: To talk about the OGY feedback control technique for systems (9), we choose $a_0 = 0.0808, b = 0.9, \alpha = 0.5896$ and $\rho = 0.1758$. In this instance, the unstable system (9) contains a single positive fixed point $(x^+, y^+) = (0.9, 1.01033)$. Following that, a matching controlled system is provided by

$$x_{n+1} = x_n + 0.4002\left((0.0808 - \ddot{\sigma}_1(x_n - 0.9) - \ddot{\sigma}_2(y_n - 1.01033))y_n - x_n + {x_n}^2 y_n\right)$$
$$y_{n+1} = y_n + 0.4002(0.9 - (0.0808 - \ddot{\sigma}_1(x_n - 0.9) - \ddot{\sigma}_2(y_n - 1.01033))y_n - {x_n}^2 y_n) \quad (31)$$

where $\tilde{K} = [\ddot{\sigma}_1 \quad \ddot{\sigma}_2]$ be the gain matrix. We get, $\tilde{A} = \begin{bmatrix} 1.3276 & 0.356498 \\ -0.7278 & 0.643502 \end{bmatrix}$, $\tilde{B} = \begin{bmatrix} 0.404333 \\ -0{,}404333 \end{bmatrix}$ and $\tilde{C} = \begin{bmatrix} 0.404333 & 0.392649 \\ -0.808666 & -0.554463 \end{bmatrix}$. It is then simple to verify that the rank of the matrix $\tilde{C}$ is 2. Consequently, the system (31) can be controlled. Afterward, the controlled system's (31) Jacobian matrix is provided by

$$\tilde{A} - \tilde{B}\tilde{K} = \begin{bmatrix} 1.3276 - 0.404333\ddot{\sigma}_1 & 0.356498 - 0.404333\ddot{\sigma}_2 \\ -0.7278 + 0.404333\ddot{\sigma}_1 & 0.643502 + 0.404333\ddot{\sigma}_2 \end{bmatrix}$$

Furthermore, the marginal stability's lines $\ddot{K}_1, \ddot{K}_2$ and $\ddot{K}_3$are given by:

$$\ddot{K}_1 = 0.113772 - 0.404333\ddot{\sigma}_1 + 0.242519\ddot{\sigma}_2 = 0$$
$$\ddot{K}_2 = 4.08487 - 0.808666\ddot{\sigma}_1 + 0.6468526\ddot{\sigma}_2 = 0$$

and

$$\ddot{K}_3 = -0.142671 + 0.161814\ddot{\sigma}_2 = 0$$

The stable triangular region for the controlled system (33) is then depicted in Fig. 7 and is bounded by the marginal lines $\ddot{K}_1, \ddot{K}_2$ and $\ddot{K}_3$.

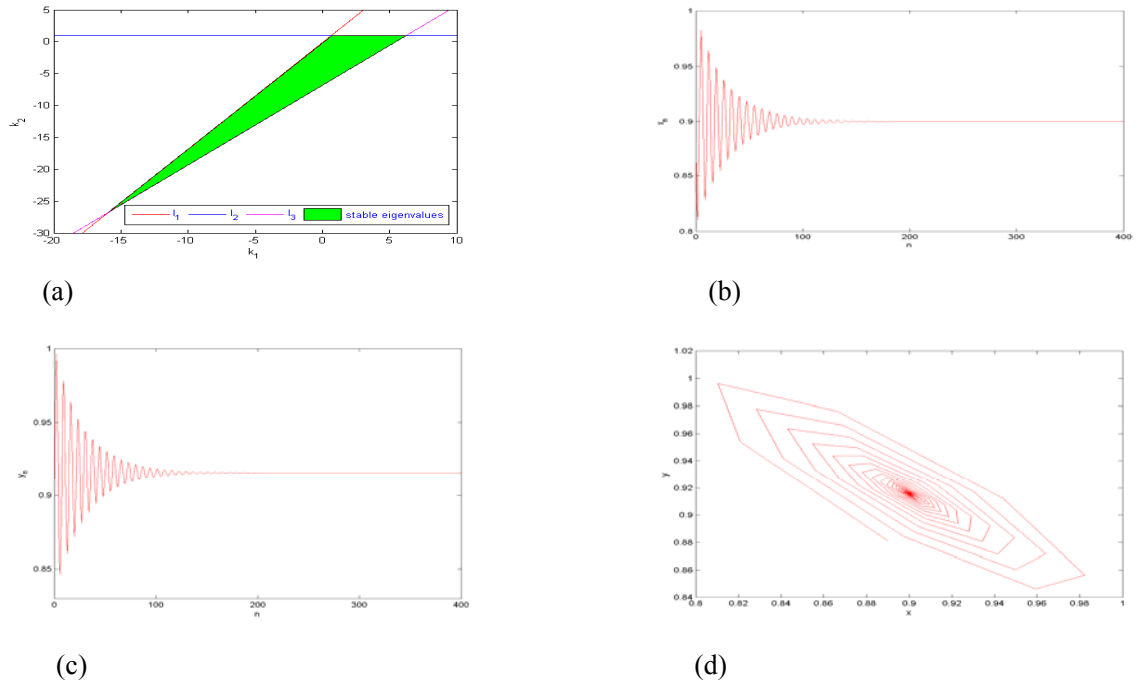

Fig. 7 Control of system (27) aberrant trajectories. (a) The $\ddot{\sigma}_1\ddot{\sigma}_2 -$ plane stability zone, (b-c) the time series for the states x and$y$, respectively, (d) Phase diagram of system (27).

6 Discussion

This study discusses a novel fractional order glycolysis model. From the Caputo fractional derivative notion, such a fractional order model is derived. By using the center manifold theorem and bifurcation theory, we demonstrate that if ρ fluctuates around the sets PD_E or NS_E, the system (9) can undergo a bifurcation (flip or NS) at a certain positive fixed point$E$.The model shows a number of complex dynamical behaviors as ρ and α are changed, such as the appearance of flip and N-S bifurcations, period-2, 4, 8, 10, 11, 14 and 16 orbits, quasi-periodic orbits, attracting invariant circle and chaotic sets. Through the calculation of maximal Lyapunov exponents and fractal dimension, we are able to affirm the presence of chaos. Additionally, we can observe that selecting the right value of ρ helps stabilize the dynamical system (9). The two bifurcations lead the system to abruptly transition from steady state to chaotic dynamical behavior via periodic and quasi-periodic states and open pathways to chaos; in other words, chaotic dynamics occur or vanish simultaneously with the formation of bifurcations. Finally, in order to remove unstable system trajectories, we employ a OGY control method. Exploring multiple parameter bifurcation in the system is still a difficult topic, though. Future research on this topic is anticipated to yield additional analytical findings.

References

Abdelaziz MAM, Ismail AI, Abdullah FA, et al. 2018. Bifurcations and chaos in a discrete SI epidemic model with fractional order. Advances in Difference Equations, 2018(44)

Ameen J, Novati P. 2017. The solution of fractional order epidemic model by implicit Adams methods. Applied Mathematical Modelling, 43: 78-84

Bagley RL, Calico R. 1991. Fractional order state equations for the control of viscoelasticallydamped structures. Journal of Guidance, Control, and Dynamics, 14(2): 304-311

Balci E, Kartal S, Ozturk I. 2021. Comparison of dynamical behavior between fractional order delayed and discrete conformable fractional order tumor-immune system. Mathematical Modelling of Natural Phenomena, 16(3)

Balci E, Ozturk I, Kartal S. 2019. Dynamical behaviour of fractional order tumor model with Caputo and conformable fractional derivative. Chaos, Solitons and Fractals, 123: 43-51

Cartwright J. 1999. Nonlinear stiffness, lyapunov exponents, and attractor dimension. Physics Letters A, 264(4): 298-302

Decroly O, Goldbeter A. 1982. Birhythmicity, chaos, and other patterns of temporal self-organization in a multiply regulated biochemical system. Proceedings of the National Academy of Sciences USA, 79: 6917-6921

Edward O, Grebogi C, Yorke JA. 1990. Controlling chaos. Physical Review Letters, 64(11): 1196-1199

Elsadany AA, Matouk AE. 2015. Dynamical behaviors of fractional-order Lotka–Volterra predator–prey model and its discretization. Journal of Applied Mathematics and Computing, 49: 269-283

Goldbeter, Lefever R. 1972. Dissipative structures for an allosteric model: Application to glycolytic oscillations. Biophysical Journal, 12(10): 1302-1315

Huang CD, Cao JD, Xiao M, Alsaedi A, Alsaadi FE. 2017. Controlling bifurcation in a delayed fractional predator–prey system with incommensurate orders. Applied Mathematics and Computation, 293: 293-310

Huang CD, Cao JD, Xiao M, Alsaedi A, Hayat T. 2017. Bifurcations in a delayed fractional complex-valued neural network. Applied Mathematics and Computation, 292: 210-227

Huang CD, Cao JD, Xiao M, Alsaedi A, Hayat T. 2018. Effects of time delays on stability and Hopf bifurcation in a fractional ring-structured network with arbitrary neurons. Communications in Nonlinear

Science and Numerical Simulation, 57: 1-13

Huang CD, MengYJ, Cao JD, Alsaedi A, Alsaadi FE. 2017. New bifurcation results for fractional BAM neural network with leakage delay. Chaos, Solitons and Fractals, 100: 31-44

Jafari H, Daftardar-Gejji V. 2006. Solving a system of nonlinear fractional differential equations using Adomian decomposition. Journal of Computational and Applied Mathematics, 196(2): 644-651

Khan, Qadeer A, Tanzeela K. 2020. Neimark‐Sacker bifurcation and hybrid control in a discrete‐time Lotka‐Volterra model. Mathematical Methods in the Applied Sciences, 43(9): 5887-5904

Khan AQ, Bukhari SAH, Almatrafi MB. 2022. Global dynamics, Neimark-Sacker bifurcation and hybrid control in a Leslie's prey-predator modelGlobal dynamics, Neimark-Sacker bifurcation and hybrid control in a Leslie's prey-predator model. Alexandria Engineering Journal, 61(12): 11391-11404

Kuznetsov Y. 2013. Elements of applied bifurcation theory (Vol. 112). Springer Science and Business Media, New York, USA

Magin R, Ortigueira MD, Podlubny I, Trujillo J. 2011. On the fractional signals and systems. Signal Processing, 91(3): 350-371

Momani S, Odibat Z. 2007. Numerical approach to differential equations of fractional order. Journal of Computational and Applied Mathematics, 96-110

Podlubny I. 1999. Fractional Differential Equations. Academic Press, New York, USA

Rana SS. 2020. Chaotic dynamics and control in a discrete-time predator-prey system with Ivlev functional response. Network Biology, 10(2): 45-61

Selkov E. 1968. Self-oscillations in glycolysis. A simple model. European Journal of Biochemistry, 4: 79-86

Wei MH, Wu JH, Guo GH. 2015. Steady state bifurcations for a glycolysis model in biochemical reaction. Nonlinear Analysis: Real World Applications, 22: 155-175

Wen G. 2005. Criterion to identify hopf bifurcations in maps of arbitrary dimension. Physical Review E, 72(2): 026201

Wolf J, Passarge J, et al. 2000. Transduction of intracellular and intercellular dynamics in yeast glycolytic oscillations. Biophysical Journal, 78(3): 1145-1153

Yao S. 2012. New bifurcation critical criterion of Flip-Neimark-Sacker bifurcations for two-parameterized family of n-dimensional discrete systems. Discrete Dynamics in Nature and Society, 2012: 264526